Load Bearing and Stiffness Tailored NiTi Implants Produced by Additive Manufacturing: A Simulation Study

Rasool Rahmanian[a], Narges Shayesteh Moghaddam[a],Christoph Haberland[a], David Dean[b], Michael Miller[b], and Mohammad Elahinia[a]

[a]University of Toledo, 2801 W Bancroft St. MS 312 Toledo, OH 43606 [a]Department of Plastic Surgery, The Ohio State University, 915 Olentangy River Road, Columbus, OH 43212 USA

ABSTRACT

Common metals for stable long-term implants (e.g. stainless steel, Titanium and Titanium alloys) are much stiffer than spongy cancellous and even stiffer than cortical bone. When bone and implant are loaded this stiffness mismatch results in stress shielding and as a consequence, degradation of surrounding bony structure can lead to disassociation of the implant. Due to its lower stiffness and high reversible deformability, which is associated with the superelastic behavior, NiTi is an attractive biomaterial for load bearing implants. However, the stiffness of austenitic Nitinol is closer to that of bone but still too high. Additive manufacturing provides, in addition to the fabrication of patient specific implants, the ability to solve the stiffness mismatch by adding engineered porosity to the implant. This in turn allows for the design of different stiffness profiles in one implant tailored to the physiological load conditions. This work covers a fundamental approach to bring this vision to reality. At first modeling of the mechanical behavior of different scaffold designs are presented as a proof of concept of stiffness tailoring. Based on these results different Nitinol scaffolds can be produced by additive manufacturing.

Keywords: Porous NiTi, Modeling

1. INTRODUCTION

Near equiatomic NiTi gets together the unique characteristics of shape memory effect and pseudoelasticity with excellent corrosion and wear resistance, high strength, as well as good biocompatibility.[1, 2]

NiTi alloys are unique among conventional biocompatible metals, because NiTi alloys shares two mechanical behaviors with actual bio material tissues.[3–5] First of all, NiTi has the recoverable strain of about 8% (due to shape memory effect and pseudoelasticity), which is similar to that of the bone (2%).[6]

Secondly, the elastic modulus of dense NiTi alloy is as low as 48GPa, which is close to that of cortical bone (12-17 GPa).[7] These two similarities as well as the similarity between the stress-strain curve of pseudoelastic NiTi and natural tissues, leads to more rapid healing time and less trauma to surrounding tissue, and makes it a good alloy for making orthopedic implants.[4]

Stiffness mismatch due to stress shielding has been identified to be the major reason for implant loosening.[8] High stiff Implant carries a considerable part of body loading placed upon it, therefore the surrounding bone would be subjected to reduced stress which may lead to bone resorption at the interface of implant-bone and eventually implant failure.[9, 10]

Despite the low stiffness of dense NiTi, it is not still at the level of cancellous bone (< 3 GPA) and even at the same level of cortical bone. By adding porosity within the implant the modulus of NiTi can even be tailored to match the modulus of cancellous bone, since the modulus decrease with increasing the porosity.[5, 11]

It has been identified that porous NiTi has better bone-ingrowth ability compare to other biocompatible porous materials.[12] Interconnecting pores and pseudoelasticity of porous NiTi implant would provide it with

Further author information: (Send correspondence to Rasool Rahmanian)
Rasool Rahmanian: E-mail: rasool.rahmanian@gmail.com, Telephone: 1 567 249 2358

Behavior and Mechanics of Multifunctional Materials and Composites 2014, edited by Nakhiah C. Goulbourne, Hani E. Naguib, Proc. of SPIE Vol. 9058, 905814
© 2014 SPIE · CCC code: 0277-786X/14/$18 · doi: 10.1117/12.2048948

Downloaded From: http://proceedings.spiedigitallibrary.org/ on 04/22/2016 Terms of Use: http://spiedigitallibrary.org/ss/TermsOfUse.aspx

pump-like and capillary properties, which can absorb body fluid required for bone ingrowth. In addition, the interconnecting pores also provide the space for tissue ingrowth and eventually bone-implant integration.[13]

There are however some disadvantages associate with long-term use of porous NiTi implants inside body. Corrosion and wear resistance decrease with adding porosity to implant due to larger surface area resulted from pores, thus Ni release would increase which may cause toxic and allergic response inside body.[14, 15] However, surface modifications, such as HA coatings, oxygen plasma immersion ion implantation, in-situ nitriding, and chemical treatment can be applied to make bio inert pore surfaces and reduce the rate of Ni release to a safe level by a factor of 3-24.[3, 16] It should be noted that strength of material of porous NiTi would reduce significantly (200-1000 MPa) , but this range is still much higher than the range of human bone (2 − 180 MPa).[17]

The main objective for using porous NiTi is tailoring the stiffness to the level of desired modulus by tuning the porosity volume percentage and its topological shape.[3] Tailored stiffness profile can be fabricated by additive manufacturing processing (AM) with different pore size (morphology) and complex implants with importing a CAD design. Selective Laser Sintering (SLS), Selective Laser Melting (SLM), laser engineered net shaping (LENS) and electron beam melting (EBM) are the most common additive manufacturing (AM) processes that use 3D CAD datas to crease three dimensional parts by fusing powders.[1] The open question is the relation between porosity with stiffness for different implant structures.

This work at the first step suggests, a topological structure for the porous material, and then simulates the behavior of the structure and compares the stiffness of the structures with different porosities.

2. MODELING

current scaffold fabrication strategies produce sub-optional porous labyrinths without natural straight edges. The biomorphic geometry that mimics the natural substrate would be one that is continuous through all space, partitioned into two not-necessarily-equal sub-spaces by a non-intersecting, two-sided surface.

The scaffold suitable for tissue engineering, in addition to be biocompatible and biodegradable, needs to satisfy the following structural configuration:

1. The scaffold architecture should be structurally and functionally biomimetic across the structural hierarchy of native cell environment.[18]
2. To mimic the multiporosity structure of the human anathomy.
3. To have the optimum surface area and pore volume. A large surface area enables cell attachment and growth, whereas a large pore volume is required to accommodate and subsequently deliver a cell mass sufficient for tissue repair.
4. The voids need to be interconnected within the scaffold. Connected pores help the material transportation and cell migration.[19]
5. Interconnected pores should be tortuous.[20, 21]
6. The aggregate of cells typically have cells separated by curved partitions. To mimic this biomorphic pattern the voids should have curved cross-sections.[22]
7. The permitability of the scaffold should be high enough to provide superior diffusion, which would facilitate the inflow of nutrients and disposal of metabolic waste.[23]

Hence, the following structure, figure 1-a, is found to satisfy the criteria as the implant. This implant has a repetitive manner, meaning that it is made up of several cells which have the same geometric shape and dimensions. Figure 1-b shows the unit cell of the implant along with the repeat directions, x, y, and z-direction.

As can be seen in the figure 1-b, the unit cell of the implant is composed of three orthogonal strands, each having 1 mm length and d mm thickness. Porosity of the structure can be tuned by changing the thickness of

Downloaded From: http://proceedings.spiedigitallibrary.org/ on 04/22/2016 Terms of Use: http://spiedigitallibrary.org/ss/TermsOfUse.aspx

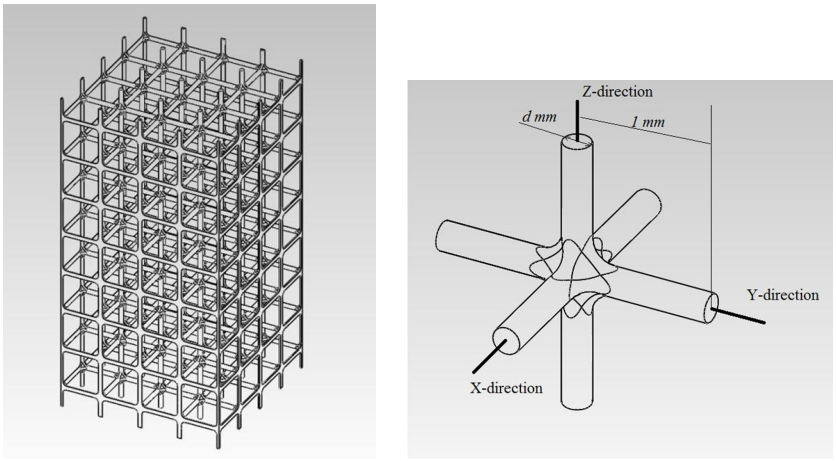

(a) (b)

Figure 1. (a) An example of the structure, made by repeating the unit-block (b) Unit cell of the structure, having strands of d millimeters, the structure could be made of this unit cell repeating itself along X, Y, and Z-direction.

each strand. For our current work the thickness of the three strands selected to be equal and vary between 0.1 and 0.7 millimeters. But it will be shown that the thickness of the strands do not need to be the same and can be different based on the stiffness demand in each direction.

This work studies the compression behavior of the implant in one direction. Since the structure is made up of the unit cells which have the same topology and dimensions, and also each unit cell is symmetric in x and y-directions, the behavior of the implant can be studied by modeling a quarter of the unit cell. Figure 2 shows the part which is selected for this study, as well as the boundary conditions on each face. As can be seen in figure 2, the compression is assumed to be in z-direction, and it is a displacement control compression, meaning that the displacement is specified on the top surface of the part, at the beginning of each step in the finite element analysis. Furthermore, since the structure is symmetric in X and Y-direction, the faces which have the normal in X and Y-directions, have X-symmetry, and Y-symmetry boundary conditions, respectively, which can be expressed in the following form:

$$\begin{aligned} \mathrm{X-symmetry} &: \quad U_x = 0, \theta_y = 0, \theta_z = 0; \\ \mathrm{Y-symmetry} &: \quad U_y = 0, \theta_z = 0, \theta_x = 0; \end{aligned}$$

Where U and θ are linear and rotational degrees of freedom respectively, and subscripts show the direction of the degree of freedom. The bottom surface is also assumed to be fixed in Z-direction.

The finite element model of the structure is made in ABAQUS, then loading steps and boundary conditions defined, and the mesh constructed in this platforms interface. Since superelastisity is not included in the material library of the software, the constitutive behavior is implemented in the user-defined interface of the ABAQUS.

Since the user interface of the ABAQUS might not be able to cover all the demands of the user, user-defined interface is also available, which lets the user, to defined customized loadings, contacts, constitutive models, and etc. in this work user-defined material subroutine `umat` is used to impalement the constitutive behavior of the SMAs into the FEA software. In the current work, The model which is used as the constitutive behavior of shape memory alloy, is developed by boyd and Lagoudas.[24]

So called Lagoudas model, firstly, selects the internal independent variables of the constitutive law, then assumes the Gibbs free energy as the potential function of the problem. Using the thermodynamics rules, then

Downloaded From: http://proceedings.spiedigitallibrary.org/ on 04/22/2016 Terms of Use: http://spiedigitallibrary.org/ss/TermsOfUse.aspx

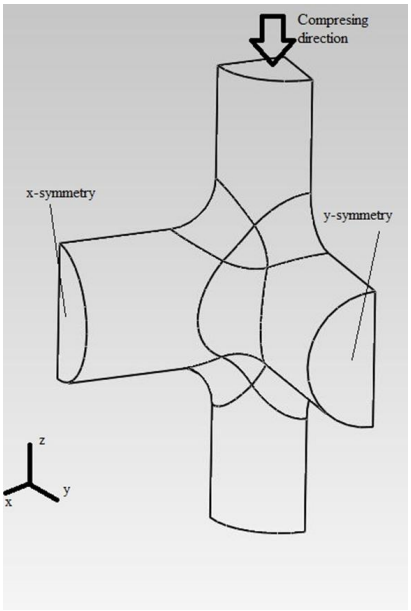

Figure 2. the CAD file which as selected to analyzed as well as the boundary conditions

they obtain the constitutive law of the shape memory alloy. The consistency of the equations then are guaranteed using Kuhn-Tucker conditions.

Qidawi and Lagoudas[25] presented implicit and explicit numerical algorithms for implementing the mathematical constitutive model. The algorithm assumes that the strain and temperature is provided at each step by the FEA software and then gives, the updated values of the internal variables at the end of each step. For the current application, the implicit algorithm, called closest point is implemented in a FORTRAN file which have the conventions of `umat`, then the properties of the model is written in the input file, and then the ABAQUS is executed according to the developed `umat`.

3. RESULTS AND DISCUSSION

In the previous part, the suggested implant presented, then the modeling procedure, constitutive law and the numerical algorithm for implementing that presented. This part mainly concerns with the results of the simulation and finding a way for tailoring stiffness to the porous structure.

First of all, as mentioned earlier, seven different structures, with seven different porosities, selected for this analysis. The diameter of the selected structures vary between 0.1 mm and 0.7 mm, which in turn results in the porosities between 98% and 32%. Since the propose is to compare the stiffness of the different structures with each other and also the dense structures, a nominal stress and strain is defined for this propose, which is the stress and strain on the imaginary unit cube which surrounds the unit cell of the structure.

As mentioned in the previous part, `umat` subroutine is used to model the constitutive behavior of the structure, and the input file of the structure is written in ABAQUS, finite element model is developed, the steps and the loading defined, and the mesh constructed on the structure, then the following properties, Table 1, assigned to the structure at the room temperature, 297 K.

The nominal stress-strain curve of seven structures, are plotted in figure 3 as well as dense structures. As can be seen, adding porosity can change the stress-strain of the material significantly. It affects the stress level, as well as the pleatu shape and the hysteresis area. Figure 4, shows one of the structures, under nominal strain of 20%, as can be seen the maximum principal strain at this instance is 23.36% which is not much higher that the nominal strain of the structure, which shows the minimal stress concentration. The other thing that needs to be pointed out is that the lateral strands do not have less contribution in carrying the longitudinal compression

Downloaded From: http://proceedings.spiedigitallibrary.org/ on 04/22/2016 Terms of Use: http://spiedigitallibrary.org/ss/TermsOfUse.aspx

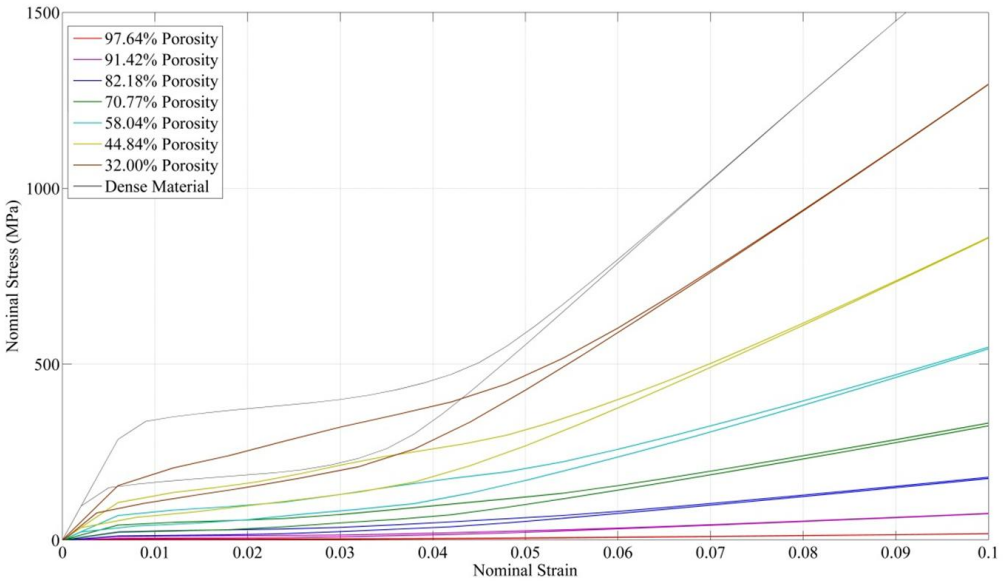

Figure 3. Nominal stress-strain curve of the unit cells, having different porosities

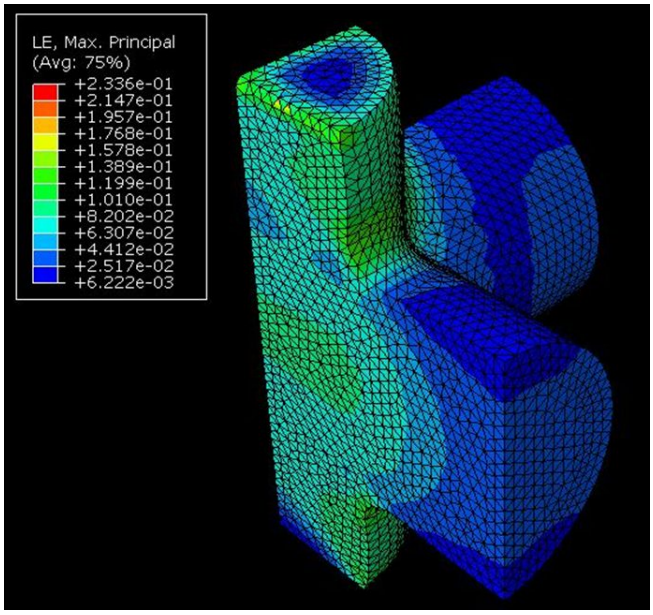

Figure 4. 3D plot of the strain distribution in the structure, nominal strain is 20%

Downloaded From: http://proceedings.spiedigitallibrary.org/ on 04/22/2016 Terms of Use: http://spiedigitallibrary.org/ss/TermsOfUse.aspx

Material Parameter	Value
Elastic stiffness of the austenite E^A	45GP A
Elastic stiffness of the martensite E^M	25GP A
Poisson's Ratio (Equal for both phases) ν	0.33
Martensitic start temperature M^{0s}	258K
Martensitic finish temperature M^{0f}	241K
Austenitic start temperature A^{0s}	273K
Austenitic finish temperature A^{0f}	283K
Maximum transformation strain H	0.03
Stress influence coefficient for austenite	-0.225MP aK^{-1}
Stress influence coefficient for martensite	-0.249MP aK^{-1}

Table 1. Material Parameters for NiTi SMA

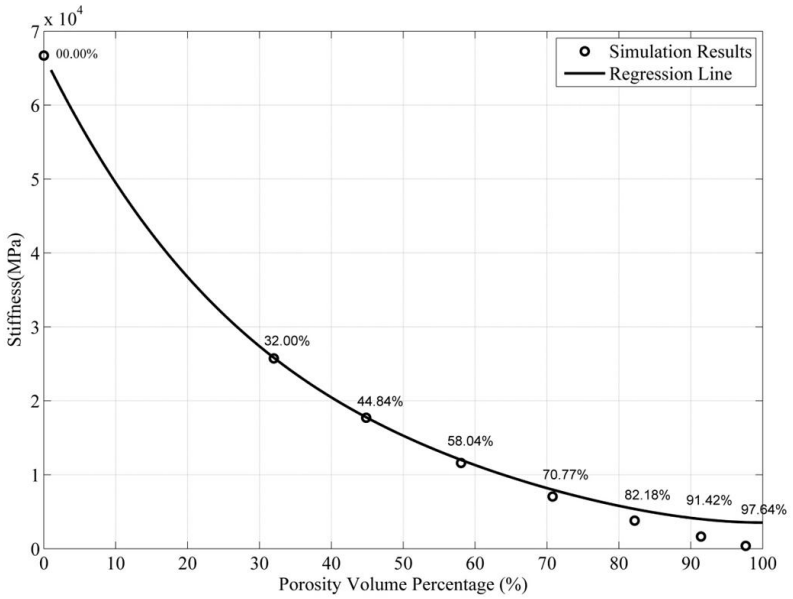

Figure 5. Stiffness of the structure against the porosity volume percentage

load, for the most of it the principal strain is less than 1%, So as mentioned earlier, the thickness of the strands can be tuned to satisfy the stiffness demand in their direction.

Figure 5 shows, the variation of stiffness against the volume percentage of porosity, it can be seen that changing the porosity of the material has a huge effect on the nominal stiffness of the material.

According to the procedure that is presented in this work, the following steps can be advised to be taken in selecting the dimensions of the suggested structure:

1. Given the stiffness in x, y, and z- direction, using table 2, find the strand diameter in each directions,
2. Given the ideal pore size, according to the osseointegration and other bio-related properties, select the unit cell size

Doing so, one can find the ideal porosity.

4. CONCLUSION

Stiffness mismatch between bone and implant is the main reason for implant failure. By adding porosity to dense NiTi, the level of stiffness would match that of cortical bone and even cancellous bone. In this study, a structure

Downloaded From: http://proceedings.spiedigitallibrary.org/ on 04/22/2016 Terms of Use: http://spiedigitallibrary.org/ss/TermsOfUse.aspx

Strand thickness (mm)	Porosity (volume percentage)	Stiffness (GPa)
0.1	97.64	0.391
0.2	91.42	1.645
0.3	82.28	3.808
0.4	70.77	7.057
0.5	58.04	11.600
0.6	44.84	17.723
0.7	32.00	25.747
Dense	00.00	66.707

Table 2. the dependency of the porosity and stiffness on the geometric dimension of the current design

for pores within NiTi implant has been suggested, and the relation between the porosity and its modulus has been identified by ABAQUS software. The results show that tailoring stiffness is possible by considering a particular porosity based on the desired modulus for implant.

5. ACKNOWLEGEMENT

The authors acknowledge the use of an Abaqus UMAT developed by Professor Lagoudas group at Texas A & M University.

REFERENCES

1. Elahinia, M. H., Hashemi, M., Tabesh, M., and Bhaduri, S. B., "Manufacturing and processing of niti implants: A review," Progress in Materials Science 57(5), 911–946 (2012).
2. Duerig, T., Pelton, A., and Stockel, D., "An overview of nitinol medical applications," Materials Science and Engineering: A 273, 149–160 (1999).
3. Bansiddhi, A., Sargeant, T., Stupp, S., and Dunand, D., "Porous niti for bone implants: a review," Acta Biomaterialia 4(4), 773–782 (2008).
4. Chu, C., Chung, C., Lin, P., and Wang, S., "Fabrication of porous niti shape memory alloy for hard tissue implants by combustion synthesis," Materials Science and Engineering: A 366(1), 114–119 (2004).
5. Greiner, C., Oppenheimer, S. M., and Dunand, D. C., "High strength, low stiffness, porous niti with superelastic properties," Acta Biomaterialia 1(6), 705–716 (2005).
6. Gjunter, V., Sysoliatin, P., and Temerkhamor, T., "Superelastic shape memory implants in maxillofacial surgery, traumatology, orthopaedics and neurosurgery," Tomsk, Russia: Tomsk University Publishing House , 15 (1995).
7. Neurohr, A. J. and Dunand, D. C., "Shape-memory niti with two-dimensional networks of micro-channels," Acta biomaterialia 7(4), 1862–1872 (2011).
8. Van Rietbergen, B., Huiskes, R., Weinans, H., Sumner, D., Turner, T., and Galante, J., "The mechanism of bone remodeling and resorption around press-fitted tha stems," Journal of biomechanics 26(4), 369–382 (1993).
9. Abdel-Hady Gepreel, M. and Niinomi, M., "Biocompatibility of ti-alloys for long-term implantation," Journal of the mechanical behavior of biomedical materials 20, 407–415 (2013).
10. Krishna, B. V., Bose, S., and Bandyopadhyay, A., "Low stiffness porous ti structures for load-bearing implants," Acta biomaterialia 3(6), 997–1006 (2007).
11. Ryan, G., Pandit, A., and Apatsidis, D. P., "Fabrication methods of porous metals for use in orthopaedic applications," Biomaterials 27(13), 2651–2670 (2006).
12. Bahraminasab, M., Sahari, B., Edwards, K., Farahmand, F., Arumugam, M., and Hong, T. S., "Aseptic loosening of femoral components–a review of current and future trends in materials used," Materials & Design 42, 459–470 (2012).

Downloaded From: http://proceedings.spiedigitallibrary.org/ on 04/22/2016 Terms of Use: http://spiedigitallibrary.org/ss/TermsOfUse.aspx

13. Zhu, S., Yang, X., Chen, M., Li, C., and Cui, Z., "Effect of porous niti alloy on bone formation: A comparative investigation with bulk niti alloy for 15 weeks in¡ i¿ vivo¡/i¿," Materials Science and Engineering: C 28(8), 1271–1275 (2008).
14. Huang, H.-H., Chiu, Y.-H., Lee, T.-H., Wu, S.-C., Yang, H.-W., Su, K.-H., and Hsu, C.-C., "Ion release from niti orthodontic wires in artificial saliva with various acidities," Biomaterials 24(20), 3585–3592 (2003).
15. Li, Y.-H., Rao, G.-B., Rong, L.-J., and Li, Y.-Y., "The influence of porosity on corrosion characteristics of porous niti alloy in simulated body fluid," Materials Letters 57(2), 448–451 (2002).
16. Li, H., Yuan, B., Gao, Y., Chung, C., and Zhu, M., "Remarkable biocompatibility enhancement of porous niti alloys by a new surface modification approach: In-situ nitriding and in vitro and in vivo evaluation," Journal of Biomedical Materials Research Part A 99(4), 544–553 (2011).
17. Li, B., Rong, L., and Li, Y., "Microstructure and superelasticity of porous niti alloy," Science in China Series E: Technological Sciences 42(1), 94–99 (1999).
18. Liebschner, M. A., "Biomechanical considerations of animal models used in tissue engineering of bone," Biomaterials 25(9), 1697–1714 (2004).
19. Mooney, D. J., Baldwin, D. F., Suh, N. P., Vacanti, J. P., and Langer, R., "Novel approach to fabricate porous sponges of poly (d, l-lactic-co-glycolic acid) without the use of organic solvents," Biomaterials 17(14), 1417–1422 (1996).
20. Mooney, D., Hansen, L., Vacanti, J., Langer, R., Farmer, S., and Ingber, D., "Switching from differentiation to growth in hepatocytes: control by extracellular matrix," Journal of cellular physiology 151(3), 497–505 (1992).
21. Ramanujan, S., Pluen, A., McKee, T. D., Brown, E. B., Boucher, Y., and Jain, R. K., "Diffusion and convection in collagen gels: implications for transport in the tumor interstitium," Biophysical journal 83(3), 1650–1660 (2002).
22. Yousaf, M. N., Houseman, B. T., and Mrksich, M., "Using electroactive substrates to pattern the attachment of two different cell populations," Proceedings of the National Academy of Sciences 98(11), 5992–5996 (2001).
23. Karande, T. S., Ong, J. L., and Agrawal, C. M., "Diffusion in musculoskeletal tissue engineering scaffolds: design issues related to porosity, permeability, architecture, and nutrient mixing," Annals of biomedical engineering 32(12), 1728–1743 (2004).
24. Boyd, J. G. and Lagoudas, D. C., "A thermodynamical constitutive model for shape memory materials. part i. the monolithic shape memory alloy," International Journal of Plasticity 12(6), 805–842 (1996).
25. Qidwai, M. and Lagoudas, D., "Numerical implementation of a shape memory alloy thermomechanical constitutive model using return mapping algorithms," International Journal for Numerical Methods in Engineering 47(6), 1123–1168 (2000).

Downloaded From: http://proceedings.spiedigitallibrary.org/ on 04/22/2016 Terms of Use: http://spiedigitallibrary.org/ss/TermsOfUse.aspx